

# Optimization of electrospun poly(*N*-isopropyl acrylamide) mats for the rapid reversible adhesion of mammalian cells

Kirsten N. Cicotte<sup>a)</sup> and Jamie A. Reed<sup>b)</sup>

*Biomedical Engineering Graduate Program, University of New Mexico, Albuquerque, New Mexico 87131; Department of Chemical and Biological Engineering, University of New Mexico, Albuquerque, New Mexico 87131; and Center for Biomedical Engineering, University of New Mexico, Albuquerque, New Mexico 87131*

Phuong Anh H. Nguyen

*Biomedical Engineering Graduate Program, University of New Mexico, Albuquerque, New Mexico 87131 and Center for Biomedical Engineering, University of New Mexico, Albuquerque, New Mexico 87131*

Jacqueline A. De Lora

*Biomedical Sciences Graduate Program, University of New Mexico Health Sciences Center and Center for Biomedical Engineering, University of New Mexico, Albuquerque, New Mexico 87131*

Elizabeth L. Hedberg-Dirk and Heather E. Canavan

*Biomedical Engineering Graduate Program, University of New Mexico, Albuquerque, New Mexico 87131; Department of Chemical and Biological Engineering, University of New Mexico, Albuquerque, New Mexico 87131; and Center for Biomedical Engineering, University of New Mexico, Albuquerque, New Mexico 87131*

(Received 1 April 2017; accepted 23 May 2017; published 13 June 2017)

Poly(*N*-isopropyl acrylamide) (pNIPAM) is a “smart” polymer that responds to changes in altering temperature near physiologically relevant temperatures, changing its relative hydrophobicity. Mammalian cells attach to pNIPAM at 37 °C and detach spontaneously as a confluent sheet when the temperature is shifted below the lower critical solution temperature (~32 °C). A variety of methods have been used to create pNIPAM films, including plasma polymerization, self-assembled monolayers, and electron beam ionization. However, detachment of confluent cell sheets from these pNIPAM films can take well over an hour to achieve potentially impacting cellular behavior. In this work, pNIPAM mats were prepared via electrospinning (i.e., espNIPAM) by a previously described technique that the authors optimized for cell attachment and rapid cell detachment. Several electrospinning parameters were varied (needle gauge, collection time, and molecular weight of the polymer) to determine the optimum parameters. The espNIPAM mats were then characterized using Fourier-transform infrared, x-ray photoelectron spectroscopy, and scanning electron microscopy. The espNIPAM mats showing the most promise were seeded with mammalian cells from standard cell lines (MC3T3-E1) as well as cancerous tumor (EMT6) cells. Once confluent, the temperature of the cells and mats was changed to ~25 °C, resulting in the extremely rapid swelling of the mats. The authors find that espNIPAM mats fabricated using small, dense fibers made of high molecular weight pNIPAM are extremely well-suited as a rapid release method for cell sheet harvesting. © 2017 American Vacuum Society. [<http://dx.doi.org/10.1116/1.4984933>]

## I. INTRODUCTION

Stimuli responsive polymers (SRPs), or smartpolymers, are polymers that can respond to changes in physical or chemical conditions by altering their properties such as shape, permeability, hydrophobicity, or color.<sup>1</sup> They have been employed by the biomedical community for many different uses including drug delivery,<sup>2</sup> tissue engineering,<sup>3,4</sup> and biosensing.<sup>5</sup> One such polymer, poly(*N*-isopropyl acrylamide) (pNIPAM or pNIPAA), has multiple biomedical applications including drug delivery, tissue engineering, and gene delivery.<sup>6</sup> pNIPAM has a unique characteristic of being a SRP that is thermoresponsive near physiologically relevant temperatures. Specifically at 37 °C, the polymer is relatively hydrophobic, and mammalian cells will readily adhere on a

substrate coated with it. By decreasing the temperature below its lower critical solution temperature (LCST) to room temperature, the polymer becomes relatively more hydrophilic. The polymer then swells, and adhered cells detach spontaneously as a confluent cell sheet.<sup>7–9</sup>

Many deposition methods for pNIPAM have been explored for use in mammalian cell culture and harvest. Depending on the application of the cells involved, the method used to deposit the pNIPAM film may be altered to achieve the desired properties such as producing cell sheets.<sup>10,11</sup> To study interactions of bacteria with pNIPAM, many groups have used self-assembled monolayers of NIPAM.<sup>12–16</sup> For tissue engineering applications, pNIPAM hydrogels have been fabricated by atom transfer radical polymerization.<sup>17</sup>

Although each of these methods produce uniform results, pNIPAM is most efficiently and reproducibly used with flat substrates, such as glass slides.<sup>7,11,18</sup> Furthermore, the above

<sup>a)</sup>K. N. Cicotte and J. A. Reed contributed equally to this work.

<sup>b)</sup>Author to whom correspondence should be addressed; electronic mail: [canavan@unm.edu](mailto:canavan@unm.edu)

techniques are dependent on using substrates with a specific surface chemistry, like glass or gold, to initiate deposition.<sup>11</sup> pNIPAM has also been previously spin-coated onto flat surfaces; however, this method can leave some areas of pNIPAM not crosslinked and, therefore, cytotoxic to cells.<sup>11,19</sup> In addition, many of these techniques have relatively slow detachment of cell sheets from pNIPAM substrates.<sup>7,18</sup> For instance, it has been reported to take up to 60 min for cell sheets to detach from a substrate.<sup>20</sup> This slow release is likely due to the limited access of hydrating water to flat 2D films, such as pNIPAM-treated Petri dishes, which results in slow swelling of the film at LCST. During these slow release times from their cell culture substrates, the cells are subjected to temperatures below their normal physiological temperatures, which may alter their behavior prior to downstream use.

It has been demonstrated that there are two methods to overcome the slow kinetics of release: (1) to provide a surface that has a high surface area to volume ratio (such as hydrogels and porous substrates) or (2) to increase the hydrophilicity of the polymer through the use of a copolymer.<sup>21</sup> To increase the surface area to volume ratio, hydrogels can be produced. Hydrogels have a larger surface area exposed to the surrounding medium rather than tethered films, allowing them to swell rapidly upon temperature shifts.<sup>22,23</sup> pNIPAM can also be copolymerized with polyethylene glycol to accelerate the hydration of hydrophilic pNIPAM chains, resulting in cell sheets that can be released in 20 min for tissue engineering applications.<sup>21</sup>

Electrospinning produces fibrous mats on the nano- to micron-size scale, which have a high surface area to volume ratio. This technique has shown great promise in artificial tissue production,<sup>24</sup> dental fillers,<sup>25</sup> textiles in wound care,<sup>26</sup> and drug delivery.<sup>27</sup> Many polymers, both natural and synthetic, have been electrospun for use as biomaterials.<sup>28–31</sup> Okuzaki *et al.* have described the ability to fabricate thermoresponsive mats using pNIPAM; however, they focused purely on the material specifications and not on the potential utility of these mats for cell culture applications.<sup>32</sup>

In this work, an alternative method for the formation of highly porous pNIPAM materials for rapid cell release was explored. Rather than treating a porous membrane with pNIPAM (which relies on the derivatization of a relatively nonreactive paper-based material with pNIPAM), porous mats composed entirely of pNIPAM via electrospinning (espNIPAM) were fabricated for the rapid release of mammalian cells. Using an electrospinning device that was built in house,<sup>28,29</sup> the production of espNIPAM mats was adapted and optimized for mammalian cell culture and rapid release of cell sheets.<sup>33</sup> To optimize pNIPAM for mammalian cell culture applications, we varied characteristics such as the molecular weight (MW) of the pNIPAM powder used, the gauge of the needle used, and the collection time (reflective of the resulting density of fibers).<sup>33</sup> Prior to their use for cell culture, the mats' chemistry, thermoresponse, and topography/morphology were assessed using scanning electron microscopy (SEM), Fourier-transform infrared spectroscopy

(FTIR), x-ray photoelectron spectroscopy (XPS), and optical and fluorescence microscopy. Subsequent to material characterization, the biocompatibility of the espNIPAM mats used for cell culture was assessed using Live/Dead and CellTracker assays, as well as detachment and readhesion studies. Two cell types were used for this assay: MC3T3-E1 cells (standard for biomaterial studies) and EMT6 cells (derived from cancerous tumors and used as tumor models).<sup>34</sup> We found that dense mats fabricated from smaller fibers of high molecular weight (HMW) pNIPAM yielded the best thermoresponse, biocompatibility, and stability in culture, as well as the most rapid release of confluent cell sheets capable of use in tissue engineering and cancer cell biology applications.

## II. MATERIALS AND METHODS

### A. Materials

All chemicals were used as received from suppliers. Poly(*N*-isopropyl acrylamide) (pNIPAM) of molecular weights 40 000 and 300 000 Da was purchased from PolySci, Inc (Warrington, PA) and Scientific Polymers (Ontario, NY), respectively. Methanol (MeOH), ACS grade, was purchased from Fisher (Pittsburgh, PA). Standard fetal bovine serum, trypsin (0.25% 1× solution, 2.5 g porcine trypsin), penicillin/streptomycin solution (10 000 units/ml penicillin; 10 000 units/ml streptomycin), and  $\alpha$ -MEM modified media were purchased from ThermoScientific HyClone (Logan, UT). MC3T3-E1 cells were purchased from ATCC® (Manassas, VA). EMT6 cells were a generous gift from James Freyer. LIVE/DEAD® for mammalian cells and CellTracker™ Green 5-chloromethylfluorescein diacetate were purchased from Invitrogen (Carlsbad, CA) and used in accordance with manufacturer's protocol. Translucent vacuum grease used to attach substrates to surfaces was obtained from Dow Corning (Midland, MI).

### B. General procedure for electrospinning

All polymer solutions were delivered at a constant rate via a New Era NE300 "Just Infusion" syringe pump (Farmingdale, NY) through a syringe fitted with a stainless steel blunt tip needle (18 g ID = 0.838 mm, 21 g ID = 0.514 mm, and 30 g ID = 0.159 mm) (Small Parts, Inc.) (Logansport, IN). The needle was charged through a high voltage supply (Glassman High Voltage, Inc. Series EL, 40–45 Watt Regulated, High Voltage DC Power, High Bridge, NJ), and the resulting polymer fibers were collected on a grounded target (6 × 6 in.<sup>2</sup> Cu plate fitted with Al foil).

### C. Electrospinning LMW and HMW pNIPAM

A 5 ml plastic syringe [inner diameter (ID) = 9.42 mm] equipped with a stainless steel blunt tip needle (18, 21, or 30 g) was used to deliver solutions of polymer dissolved in methanol (MeOH) (10 and 20 wt. %) at a volumetric flow rate of 3.5 ml/h and a voltage difference of 1 kV/cm from the needle tip to the collection plate. The grounded Cu collection

plate was fitted with aluminum foil. Upon spinning, the foil containing the newly spun mat was removed and mats were removed from the Cu target and dried *in vacuo* overnight, to ensure the removal of any residual MeOH.

#### D. Scanning electron microscopy

SEM analysis was performed using a Zeiss Supra 55VP Field Emission Gun SEM (Peabody, MA). The samples were sputter coated with AuPd in an Edwards S150B sputter coater (Crawley, West Sussex, UK) for 12 s. Imaging was performed with an acceleration voltage using SmartSEM software provided by Zeiss (Peabody, MA). Image analysis utilized IMAGE J (NIH) (Bethesda, MD) to determine the diameter of fibers in the mats.

#### E. X-ray photoelectron spectroscopy

XPS survey and high resolution spectra were obtained at the University of Washing using a Kratos Axis Ultra spectrometer (Chestnut Ridge, NY) with a monochromatic Al K $\alpha$  (1486.6 eV) source at 225 W. High-resolution spectra of carbon and oxygen were obtained ( $n=5$ ) for low molecular weight (LMW) and HMW espNIPAM mats. Survey spectra were obtained at a pass energy of 80 eV and high-resolution spectra at a pass energy of 20 eV. The base pressure was less than  $5 \times 10^{-9}$  Torr. Charge compensation was accomplished using low energy electrons. Linear background was used for elemental quantification of C1s.

CASAXPS software (Manchester, UK) was used to analyze data. Core-level spectral peaks were fitted using the minimum number of peaks possible to obtain random residuals. A 70% Gaussian/30% Lorentzian line shape was used to fit the peaks, and a linear function was used to model the background.

#### F. Fourier transform infrared

Sample preparation for pNIPAM included making a 1 mg/ml solution in methanol (MeOH) and drop casting the solution on a KBr plate (Aldrich) (St. Louis, MO), and for electrospun mats (espNIPAM), the spectra were recorded as spun (neat). FTIR data were obtained using a Nicolet<sup>TM</sup> 6700 FTIR (Thermo Electron Corporation) (Waltham, MA) equipped with a continuum microscope. OMNIC<sup>TM</sup> software (ThermoScientific) (Waltham, MA) parameters included selecting a transmission ESP accessory, a detector (DTGS KBr) and a beamsplitter (XT-KBr) (Waltham, MA).

Data were collected for 64 scans at a resolution of 4, from 400 to 4000  $\text{cm}^{-1}$ . Spectra were exported as an .asc file and analyzed in Excel (Microsoft Corp.) (Redmond, WA). All spectra were normalized to the C=O stretching at 1640  $\text{cm}^{-1}$ .

#### G. Thermoresponse

The thermoresponse of the mats was tested using a CO<sub>2</sub> microscope stage incubator from Okolab (Naples, Italy). Using the OKOLAB software, the temperature of the stage

incubator was held constant at temperatures ranging from 26 to 40 °C. Within the incubator, mats were exposed to DI water and observed using a light microscope (Nikon F100, Melville, NY) equipped with a 10 $\times$  objective.

#### H. Cell culture

Mammalian cell culture of murine osteoblastic cell line MC3T3-E1 cells and EMT6 cells followed techniques we previously established for mammalian cell culture on plasma polymerized NIPAM.<sup>7,9,32</sup> Briefly, the cells were cultured in T-75 tissue cultured polystyrene (TCPS) flasks using  $\alpha$ -MEM modified (MC3T3-E1) or DMEM (BAECs) media supplemented with 10% (v/v) fetal bovine serum and 1% (v/v) penicillin/streptomycin, at 37 °C and 5% CO<sub>2</sub> with a relative humidity of 95%. Once cells were 70%–90% confluent, they were lifted using trypsin for seeding.

#### I. Cytotoxicity of pNIPAM

Cytotoxicity tests are used to determine if components from the pNIPAM surface are leaching into the medium. In this case, espNIPAM mats were submerged in the normal growth medium for 24 h and incubated at cell growth conditions. The treated medium was then collected. Simultaneously, cells were grown at normal conditions until  $\sim$ 60% confluent. The medium on these cells was replaced with 100%, 10%, 1%, and 0% treated media. The cells were then cultured for another 24 h in the treated medium to determine if anything leached from the substrate that could impart cytotoxicity to the cultured cells.<sup>33</sup> Cell viability was determined using a commercial LIVE/DEAD for mammalian cell fluorescence assay from Invitrogen. To verify the results, live controls (0% treated media) and dead controls (incubated in 0% treated media, followed by incubation in 70% methanol for 1 h) were used for comparison.

#### J. Staining of cells

Prior to use, the stock solution of CellTracker was thawed and a 25  $\mu\text{m}$  solution in serum free media is prepared. This solution replaced the media in the flask of confluent cells. The probe was incubated with the cells at cell culture conditions for 60 min and then replaced with normal growth media for 30 min. The cells were then rinsed with DPBS and harvested.

#### K. Transfer of harvested cells

To determine whether the espNIPAM mats formulated under the different conditions were thermoresponsive, cells were reversibly adhered using a slight variation of a previously described technique.<sup>7</sup> Briefly, cells were cultured to confluence ( $\sim$ 4 days). The medium was removed and replaced with serum-free media at 4 °C to begin cell release. A poly(vinylidene fluoride) (PVDF) membrane from Millipore (Billerica, MA) was used as a superstrate to aid in the transfer of cells.<sup>35</sup> The medium was removed until there was only a thin film on the cells. A sheet of PVDF was laid



on top of the cell sheet, and the plate was incubated at 37 °C for 30 min, to allow the cells to attach to the PVDF. Serum-free media at 4 °C were added to each well since a previous investigation indicated that this facilitated the fastest release from pNIPAM.<sup>7</sup> The culture plate was then placed on a shaker platform for 30 min, at which point the PVDF was slowly peeled from the substrate with the cells, and moved to a new TCPS well. After 30 min of incubation at 37 °C, the PVDF was carefully peeled away from the cells. Cells were monitored for 24 h.

### III. RESULTS

#### A. Preparation of mats

It was previously demonstrated that fibrous mats of pNIPAM could be electrospun.<sup>18</sup> In that work, the fabrication process of espNIPAM was the focus of the project using a singular set of parameters (polymer concentration versus voltage). In the current work, we optimized this technique to create espNIPAM mats for mammalian cell culture by adapting a number of conditions including: MW, needle gauge

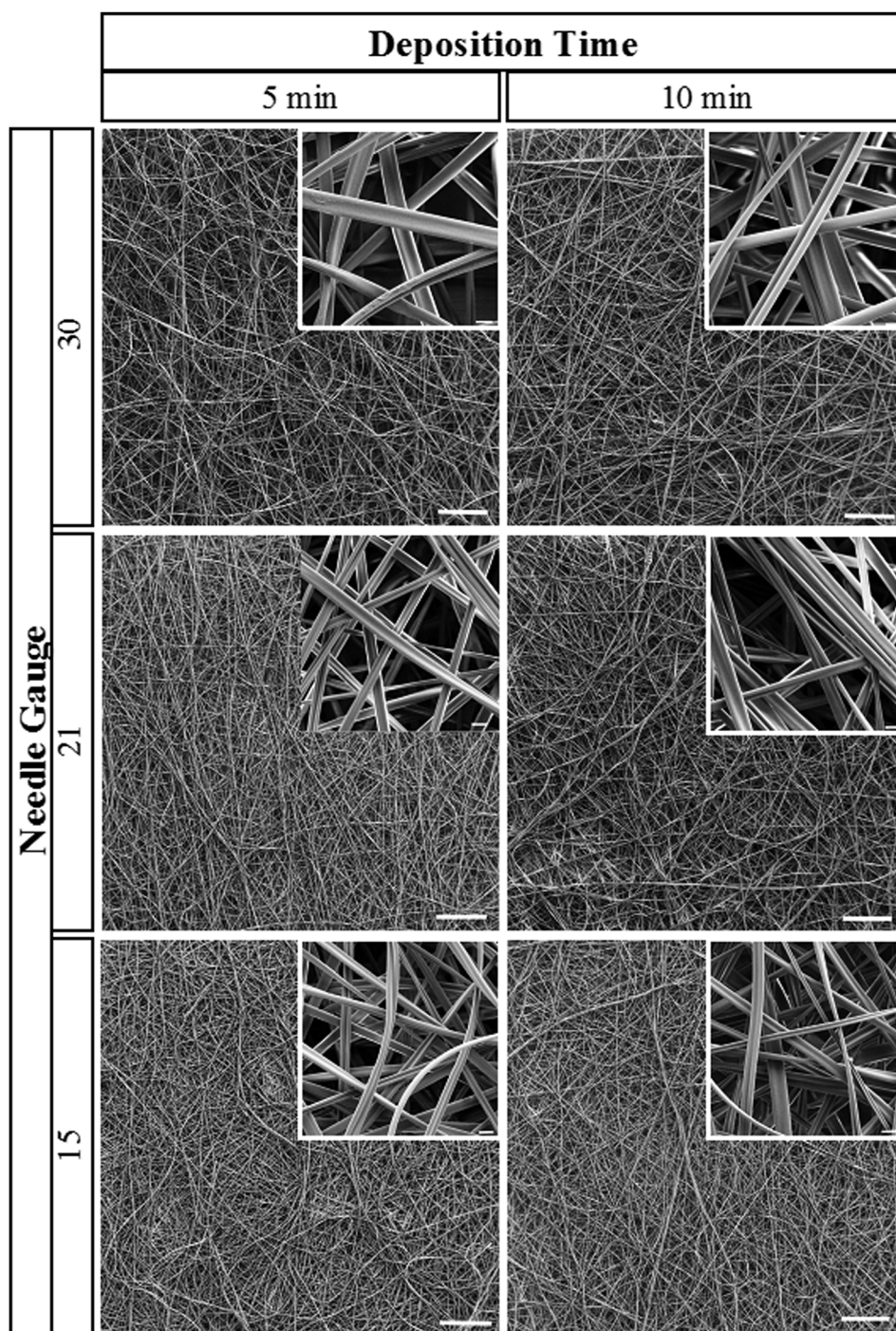


FIG. 1. SEM images of espNIPAM mats spun for 5 (left) or 10 (right) min, using a 15 (bottom), 21 (middle), or 30 (top) gauge needle. Scale bars are 100  $\mu\text{m}$  for the unmagnified images and 2  $\mu\text{m}$  for the inset magnified images.

size, and mat collection time. These parameters were chosen as they have been shown to affect the mat density and the fiber size, which are important considerations when using the mats for cell culture.<sup>33</sup> Previous work with pNIPAM electrospun mats has primarily used pNIPAM with copolymers as a thermoresponsive drug delivery system<sup>36–40</sup> with few studies examining espNIPAM's capability for mammalian cell culture and cell sheet production.<sup>41</sup>

We found that uniform, “dog bone”-shaped fibers with a diameter of  $<1\ \mu\text{m}$  were generated from each of the variations in the technique, as shown in the SEM images (see Fig. 1). In particular, there appeared to be no statistical difference in the fiber diameter regardless of the needle gauge. Fiber diameters resulting from 18, 21, and 30 needle gauge diameters, as measured using IMAGE J from SEM images, indicate that neither the gauge size nor the density of fibers (as controlled by collection time) significantly affects the fiber diameter. The fiber diameters range from  $0.9$  to  $1.15\ \mu\text{m} \pm 0.5$ . However, the mat thickness was found to depend linearly on the collection time: by increasing collection time from 5 to 10 min, the mat thickness increased from 12 to  $24\ \mu\text{m}$ .

## B. Chemical composition of mats

To ensure that the espNIPAM fibers had the same chemistry as their powdered pNIPAM precursor, FTIR and XPS were performed on each of the LMW and HMW powder, as well as on the spun mat (see Fig. 2). The close observation of FTIR spectra generated from the three samples shows that the characteristic functional groups of pNIPAM are present in all the three samples. For instance, C=O stretching at  $\sim 1645\text{ cm}^{-1}$ , CH<sub>3</sub> asymmetric stretching at  $\sim 2970\text{ cm}^{-1}$ , and N-H stretching at  $\sim 3301\text{ cm}^{-1}$  are present in all three spectra (indicated by peaks with red stars).<sup>42</sup> A difference in the three spectra is the relatively high background noise of the espNIPAM mat, which can be attributed to the thickness of the sample. These results indicate that the bulk of the

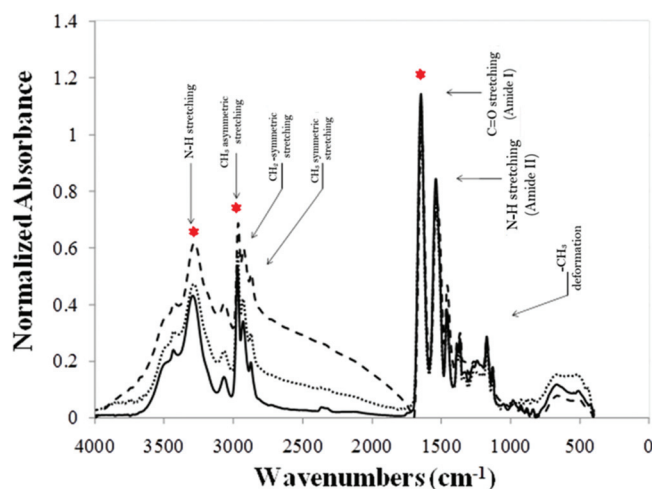


FIG. 2. FTIR spectra of HMW (small dashed lines) and LMW (large dashed lines) pNIPAM powders as well as a HMW espNIPAM mat (solid line). All samples have the expected stretches characteristic of pNIPAM, as previously reported by Pan *et al.*

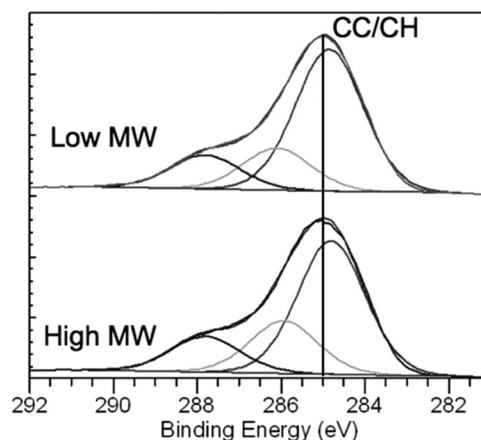


FIG. 3. High resolution C1s spectra of low (top) and high (bottom) molecular weight espNIPAM mats. Amide (O=C-N; 288 eV) and amine (C-N; 286 eV) peaks characteristic of pNIPAM are present in both formulations.

espNIPAM mats' chemistry closely resembles that of its powdered pNIPAM precursor, and thus, the processing of the mats has not significantly altered the resulting chemistry.

To confirm the chemistry of the espNIPAM mats, they were also analyzed using XPS. As the size of the fibers generated using each of the needles is on the order of a micron, it is well below the resolution of the XPS;<sup>9</sup> therefore, the mats generated using different needle sizes were not studied using this technique. As shown in Table I and Fig. 3, the mats generated from HMW pNIPAM were 78.6% C, 11.3% N, and 10.1% O, whereas mats generated from LMW pNIPAM were 79.0% C, 10.2% N, and 10.8% O. These results are within the experimental error of the instrument ( $\sim 2\%$ – $5\%$ )<sup>9,17</sup> and are consistent with the structure predicted by the stoichiometry of the NIPAM monomer (75% C, 12.5% O, and 12.5% N).<sup>9</sup> In addition, these results are consistent with pNIPAM mats created from other standard deposition techniques (such as plasma polymerization) that yield thermoresponsive substrates capable of supporting reversible cell adhesion.<sup>18,19,43–46</sup> Observation of the high resolution C1s spectra further confirms that the electrospun mats have the same chemical species as pNIPAM, including hydrocarbon (at 285 eV), as well as equal amounts of amine and amide characteristics (at +1.5 and 3.0 eV), further confirming that the electrospinning process has not altered the polymer (see Fig. 3).

## C. Thermoresponse of mats

Having established that espNIPAM mats generated from HMW and LMW pNIPAM retained the proper chemistry, they were tested to ensure that thermoresponsive characteristics were retained. As the topography of the mats varies widely due to the overlapping fibers that make up the mat, contact angle goniometry was not a suitable technique for the observation of the mats' thermoresponse. Instead, the mats were held stable at temperatures ranging from 40 to  $26^\circ\text{C}$  and imaged using an inverted optical microscope (see Fig. 4). It was found that the mats created from LMW pNIPAM were



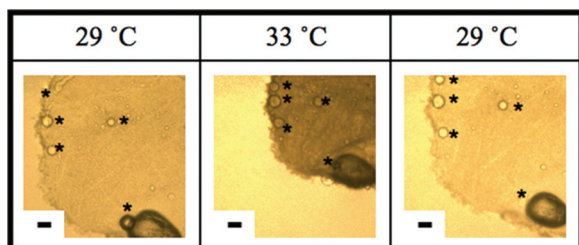


FIG. 4. Bright field microscopy images of an espNIPAM mat at the temperatures it is subjected to cycles above and below the LCST. The mat is initially below the LCST (29 °C, left), collapsing when the temperature changes to above the LCST (33 °C, middle). When the temperature is lowered below the LCST again (right), the mat reversibly swells. Asterisks near air bubbles in the mat are included to provide the point of reference. A video illustrating this reversible behavior is included in the supplementary material. The scale bar is 100  $\mu\text{m}$ .

not stable, dissolving immediately in water. Such behavior would render mats created from LMW pNIPAM useless for cell culture, which is dependent upon aqueous media. However, the mats formed from the HMW pNIPAM were stable in the solution and demonstrated reversible thermoresponses [see Fig. 4(b) as well as a video in the supplementary material].<sup>56</sup> Upon hydration above the LCST ( $\sim 31^\circ\text{C}$ ), the HMW espNIPAM mats originally collapsed but rapidly (within 5 min) swelled when the temperature shifted below the LCST. These results indicate that the HMW espNIPAM mats are more useful for reversible cell attachment.

#### D. Cytotoxicity of espNIPAM

There are conflicting claims in the literature as to whether the method used to fabricate pNIPAM substrates influences their resulting biocompatibility.<sup>11,47–50</sup> We recently demonstrated that although the NIPAM monomer is cytotoxic, the primary techniques used to create pNIPAM mats are stable and nontoxic.<sup>19</sup> To be diligent, the espNIPAM mats generated were assessed for their potential cytotoxicity (or biocompatibility). This process includes incubating the mat in normal growth media at cell culture conditions for 24 h in order to identify whether there are any substances that may leach into the media, interfering with cell viability and proliferation.<sup>19</sup> These treated media replace media on cells that are  $\sim 60\%$  confluent. After 24 h of exposure to the treated media, cells exposed to HMW pNIPAM remained 99% viable and proliferated [see Fig. 5(b)]. In contrast, those cells that were

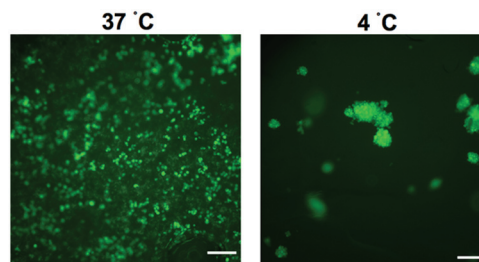


FIG. 6. Fluorescence microscopy image of 3T3 cells tagged with CellTracker. This marker allowed imaging of live cells through the opaque espNIPAM mat. Images of 3T3 cells adhered to HMW espNIPAM mats were obtained above the LCST (left) and after the cells have detached below the LCST (right). The scale bar is 100  $\mu\text{m}$ .

exposed to LMW were no longer viable, as evidenced by the red color when imaged [see Fig. 5(a)]. From these results, we conclude that the HMW mats are not toxic to the cells and can be used for rapid cell detachment experiments.

#### E. Cell response/detachment

Since their introduction in the mid-1990s for use in culturing mammalian cells, over 60 different cell lines have appeared in the literature on pNIPAM substrates. For this study, EMT6 and MC3T3-E1 were chosen. MC3T3-E1 (3T3) cells are standard for biomaterial studies and have been successfully detached from pNIPAM in the previous literature;<sup>51</sup> EMT6 cells are tumor-derived (cancerous), which have also been used in previous studies using pNIPAM.<sup>52</sup> Both cells show no adverse reaction to the polymer and have been used for tumor models.<sup>34</sup>

Initially, cells were seeded onto the mats at a high ratio (100 000 cells/well for 3T3s and 50 000 cells/well for EMT6) to ensure cell attachment and rapid cell proliferation. As it was extremely difficult to visualize the cells on the mats in their collapsed (i.e., opaque) state, the observation of cellular behavior was achieved using fluorescence microscopy (using CellTracker) on the mats 24 h after seeding, as shown in Fig. 6. The temperature was then shifted below the LCST by exchanging the media with 4 °C media to determine if the cells would detach from the mats.

Figure 6 illustrates that, once exposed to temperatures below the LCST of the polymer, the cells detached from their espNIPAM mat substrates. Interestingly, although both the cancerous EMT-6 and noncancerous 3T3 cells readily

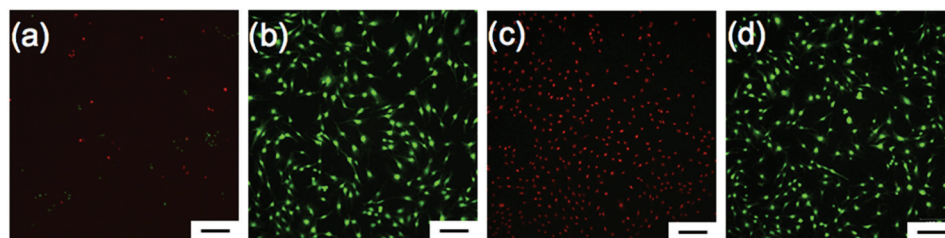


FIG. 5. Fluorescence microscopy images of 3T3 cells stained with LIVE/DEAD after exposure to 100% LMW (a) and HMW (b) treated media for 24 h, as well as dead (c) and live (d) controls. Cells remain viable when exposed to the HMW polymer, verifying that it is not cytotoxic, whereas the cells exposed to the LMW polymer are not viable after 24 h. The scale bar is 100  $\mu\text{m}$ .

TABLE I. Relative atomic percentages of HMW and low (LMW) espNIPAM mats as measured by XPS. The theoretical composition of pNIPAM is provided for comparison.  $n = 5$  and standard deviation  $< 1$ .

Formulation	Relative atomic %		
	C	N	O
HMW	78.6	11.3	10.1
LMW	79.0	10.2	10.8
Theoretical	75.0	12.5	12.5

attached to the mats, the noncancerous 3T3 cells attached but did not form cell “sheets.” It is also interesting to note that a disparity in the adhesion and proliferation of these cell types has not been previously observed for other derivatization techniques, such as solution deposition and plasma polymerization.<sup>7,18</sup> This finding is likely due to 3T3’s sensitivity to contact inhibition of cell division.<sup>53</sup> In other NIPAM deposition techniques, 3T3 only recognizes other 3T3 cells. With espNIPAM mats, 3T3 may be recognizing espNIPAM fibers as nearby cells, a concept that will be further studied. Finally, this method yielded much faster cell release than many other methods reported in the literature: 80% of the cells detached within 5 min from the mats when the temperature was shifted below the LCST (as opposed to 60 min or several hours).<sup>20</sup>

Due to their rapid growth, the cancerous EMT6 cells were used in the remaining experiments to determine which characteristics of the mats would support cell sheet attachment/detachment. Although it was established using SEM that the gauge diameter did not change the size distribution of the resulting fibers within espNIPAM mats (see Table I), the mats produced using a 30 gauge needle supported cell sheets more consistently. These results are consistent with previous work, indicating that dense, small fibers create a mat that has a lower interfiber distance, thus minimizing cell penetration into the mat, forming a mat that is perceived by the cells as a 2D substrate, and supporting cell sheet formation.<sup>54</sup>

## F. Cell response/transfer

Having demonstrated that the cell sheets were easily released in an unassisted manner from espNIPAM mats generated from HMW pNIPAM (i.e., “popped off”), we tested the ability to relocate the cell sheet into a new well using a PVDF superstrate (i.e., “lift off”). To achieve assisted cell transfer, a PVDF superstrate was attached to the apical surface of EMT6 cells cultured atop espNIPAM mats.<sup>55</sup> As a negative control, the same procedure was attempted using a PVDF membrane to transfer replicate cells cultured atop blank TCPS (no pNIPAM). The temperature was changed below the LCST, and the membranes were removed from the well, with cells still attached to the membrane. These cells were relocated into a new TCPS well, after which the PVDF membrane was removed. The cells were imaged 24 h after their transfer to assess their attachment and proliferation.

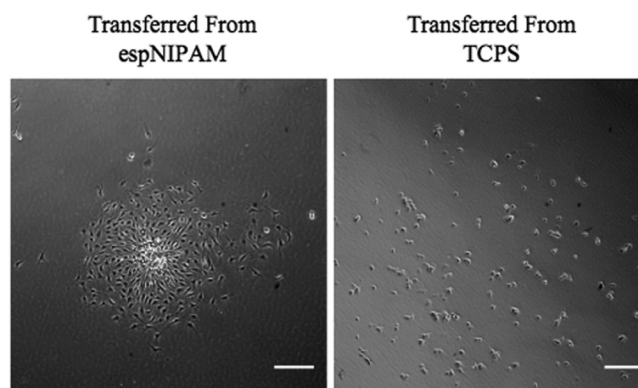


FIG. 7. Bright field microscopy image of EMT6 cells that have been transferred to a new well with PVDF superstrates from thermoresponsive HMW espNIPAM mats (left) and control TCPS (right). Cells detached from the espNIPAM mats rapidly adhere to their new culture substrate after being transferred, as opposed to those from the control substrate. This indicates that the cells released from HMW espNIPAM mats retained their extracellular matrix. The scale bar is 100  $\mu\text{m}$ .

As shown in Fig. 7, the cells that were detached from the espNIPAM mats using PVDF readily attached to their new TCPS substrate. In contrast, the cells that were removed from the negative control (blank TCPS wells) using PVDF did not attach to a new culture substrate after 24 h of relocation. These results are consistent with previous indications that when cells detached from pNIPAM mats, their ECM remains intact and promotes the adhesion of the cells to their new culture substrate.<sup>7,43–45</sup> However, those previous studies employed NIPAM deposition techniques such as plasma polymerization and electron beam ionization for the fabrication of pNIPAM mats, which are more expensive to build and characterize and traditionally require 60 min to achieve the detachment of similarly sized cell sheets.<sup>20</sup>

## IV. CONCLUSIONS

In this work, we optimized a technique capable of electrospinning highly porous, biocompatible, and thermoresponsive pNIPAM substrates capable of reversibly adhering mammalian cells. A number of parameters used during electrospinning were varied (e.g., the collection time, needle gauge size, and MW of the pNIPAM powder used), and the resulting espNIPAM mats were characterized using a variety of techniques to assess their thermoresponse, chemistry, and biocompatibility. Interestingly, we found that, regardless of the gauge of the needle used when spinning the mat, similar fiber distribution was produced. It was demonstrated that espNIPAM mats generated using this technique retain the same chemistry as the pNIPAM powder, as well as its reversibly thermoresponsive behavior near physiologically relevant temperatures. Although both LMW and HMW pNIPAM powders were capable of producing espNIPAM mats, due to concerns over cytotoxicity and complete collapse of LMW espNIPAM mats, only the HMW espNIPAM mats were appropriate for mammalian cell culture.

Using EMT6 cells, it was shown that small, dense fibers better supported cell sheet formation and vastly improved

the speed of detachment: an impressive 80% of these cancerous cells detached within 5 min from the mats when the temperature was shifted below the LCST (as opposed to 60 min). This indicates that mats generated using these parameters will be ideal for cell sheet engineering and cancer cell biology studies, as detaching cells will be exposed to an artificially low temperature for a shorter time frame during detachment (which could, in turn, decrease the effect on cellular processes prior to their analysis downstream).

## ACKNOWLEDGMENTS

The authors wish to thank Brissa Ponce and Jim Freyer for their assistance and useful discussions. The authors also thank Michael Brumbach (XPS) and Bonnie Mckenzie (SEM) at Sandia National Labs for data acquisition. This work was funded by the NSF-Partnership for Research and Education in Materials (PREM) program Grant No. DMR-0611616 and NIBIB Grant No. EB-002027, as well as funding from the UNM Center for Biomedical Engineering. In addition, J.A.R. was supported by the NIH Ruth Kirschstein National Research Service Award.

- <sup>1</sup>A. Lendlein and V. P. Shastri, *Adv. Mater.* **22**, 3344 (2010).
- <sup>2</sup>W. Cheng, L. Gu, W. Ren, and Y. Liu, *Mater. Sci. Eng., C* **45**, 600 (2014).
- <sup>3</sup>J. Hu, H. Meng, G. Li, and S. I. Ihekwe, *Smart Mater. Struct.* **21**, 53001 (2012).
- <sup>4</sup>A. S. Hoffman, *Adv. Drug Delivery Rev.* **65**, 10 (2013).
- <sup>5</sup>N. S. Terefe, O. Glagovskaia, K. De Silva, and R. Stockmann, *Food Bioprod. Process.* **92**, 208 (2014).
- <sup>6</sup>M. A. Ward and T. K. Georgiou, *Polymers* **3**, 1215 (2011).
- <sup>7</sup>J. A. Reed, A. E. Lucero, S. Hu, L. K. Ista, M. T. Bore, G. P. López, and H. E. Canavan, *ACS Appl. Mater. Interfaces* **2**, 1048 (2010).
- <sup>8</sup>H. E. Canavan, X. Cheng, D. J. Graham, B. D. Ratner, and D. G. Castner, *Plasma Processes Polym.* **3**, 516 (2006).
- <sup>9</sup>B. D. Ratner, A. S. Hoffman, F. J. Schoen, and J. E. Lemons, *Biomaterials Science*, 3rd ed. (Academic, Cambridge, MA, 2012).
- <sup>10</sup>R. M. P. da Silva, J. F. Mano, and R. L. Reis, *Trends Biotechnol.* **25**, 577 (2007).
- <sup>11</sup>M. A. Cooperstein and H. E. Canavan, *Langmuir* **26**, 7695 (2010).
- <sup>12</sup>A. Leon De and R. C. Advincula, *ACS Appl. Mater. Interfaces* **6**, 22666 (2014).
- <sup>13</sup>S. Mendez, L. K. Ista, and G. P. Lo, *Biofouling* **26**, 111 (2010).
- <sup>14</sup>L. K. Ista, S. Mendez, H. Pe, and G. P. Lo, *Langmuir* **17**, 2552 (2001).
- <sup>15</sup>H. Gu and D. Ren, *Front. Chem. Sci. Eng.* **8**, 20 (2014).
- <sup>16</sup>S. J. Lee *et al.*, *J. Mater. Chem. B* **3**, 5161 (2015).
- <sup>17</sup>A. Galperin, T. J. Long, S. Garty, and B. D. Ratner, *J. Biomed. Mater. Res., Part A* **101**, 775 (2013).
- <sup>18</sup>J. A. Reed, S. A. Love, A. E. Lucero, C. L. Haynes, and H. E. Canavan, *Langmuir* **28**, 2281 (2012).
- <sup>19</sup>M. A. Cooperstein and H. E. Canavan, *Biointerphases* **8**, 19 (2013).
- <sup>20</sup>N. G. Patel and G. Zhang, *Organogenesis* **9**, 93 (2013).
- <sup>21</sup>Z. Tang, Y. Akiyama, and T. Okano, *Polymers* **4**, 1478 (2012).
- <sup>22</sup>N. S. Rejinold, T. Baby, K. P. Chennazhi, and R. Jayakumar, *Colloids Surf. B* **114**, 209 (2014).
- <sup>23</sup>J. F. Pollock and K. E. Healy, *Acta Biomater.* **6**, 1307 (2010).
- <sup>24</sup>F. Ozcan, S. Ertul, and E. Maltas, *Mater. Lett.* **182**, 359 (2016).
- <sup>25</sup>S. B. Qasim, S. Najeeb, R. M. Delaine-Smith, A. Rawlinson, and I. Ur Rehman, *Dent. Mater.* **33**, 71 (2017).
- <sup>26</sup>P. Peh, N. S. J. Lim, A. Blocki, S. M. L. Chee, H. C. Park, S. Liao, C. Chan, and M. Raghunath, *Bioconjugate Chem.* **26**, 1348 (2015).
- <sup>27</sup>C. H. Huang, C. Y. Chi, Y. S. Chen, K. Y. Chen, P. L. Chen, and C. H. Yao, *Mater. Sci. Eng., C* **32**, 2476 (2012).
- <sup>28</sup>E. Hedberg-Dirk, K. Cicotte, and S. Dirk, *MRS Proc.* **1239**, VV05-02 (2011).
- <sup>29</sup>K. Cicotte, E. Hedberg-Dirk, and S. M. Dirk, *J. Appl. Polym. Sci.* **117**, 1984 (2010).
- <sup>30</sup>W. Ji, Y. Sun, F. Yang, J. J. P. van den Beucken, M. Fan, Z. Chen, and J. A. Jansen, *Pharm. Res.* **28**, 1259 (2011).
- <sup>31</sup>Y. Sharma, A. Tiwari, S. Hattori, D. Terada, A. K. Sharma, M. Ramalingam, and H. Kobayashi, *Int. J. Biol. Macromol.* **51**, 627 (2012).
- <sup>32</sup>H. Okuzaki, K. Kobayashi, and H. Yan, *Synth. Met.* **159**, 2273 (2009).
- <sup>33</sup>D. N. Rockwood, D. B. Chase, R. E. Akins, and J. F. Rabolt, *Polymer* **49**, 4025 (2008).
- <sup>34</sup>J. Freyer, *J. Cell Physiol.* **176**, 138 (1998).
- <sup>35</sup>A. Kushida, M. Yamato, C. Konno, A. Kikuchi, Y. Sakurai, and T. Okano, *J. Biomed. Mater. Res.* **51**, 216 (2000).
- <sup>36</sup>J. Hu, H. Y. Li, G. R. Williams, H. H. Yang, L. Tao, and L. M. Zhu, *J. Pharm. Sci.* **105**, 1104 (2016).
- <sup>37</sup>H. Priya James, R. John, and A. Alex, *Acta Pharm. Sin. B* **4**, 120 (2014).
- <sup>38</sup>M. Chen, Y.-F. Li, and F. Besenbacher, *Adv. Healthcare Mater.* **3**, 1721 (2014).
- <sup>39</sup>T. Tran, M. Hernandez, D. Patel, and J. Wu, *Adv. Mater. Sci. Eng.* **2015**, 180187.
- <sup>40</sup>Y.-Y. Li, X.-Z. Zhang, H. Cheng, J.-L. Zhu, U.-N. Li, S.-X. Cheng, and R.-X. Zhuo, *Nanotechnology* **18**, 505101 (2007).
- <sup>41</sup>S. Rayatpisheh, D. E. Heath, A. Shakouri, P. O. Rujitanaroj, S. Y. Chew, and M. B. Chan-Park, *Biomaterials* **35**, 2713 (2014).
- <sup>42</sup>Y. V. Pan, R. A. Wesley, R. Luginbuhl, D. D. Denton, and B. D. Ratner, *Biomacromolecules* **2**, 32 (2001).
- <sup>43</sup>H. E. Canavan, *J. Appl. Biomater. Biomech.* **6**, 81 (2008), available at <https://www.ncbi.nlm.nih.gov/pmc/articles/PMC3842098/>.
- <sup>44</sup>H. E. Canavan, D. J. Graham, X. Cheng, B. D. Ratner, and D. G. Castner, *Langmuir* **23**, 50 (2007).
- <sup>45</sup>X. Cheng, H. E. Canavan, M. J. Stein, J. R. Hull, S. J. Kweskin, M. S. Wagner, G. A. Somorjai, D. G. Castner, and B. D. Ratner, *Langmuir* **21**, 7833 (2005).
- <sup>46</sup>B. M. Bluestein, J. A. Reed, and H. E. Canavan, *Appl. Surf. Sci.* **392**, 950 (2017).
- <sup>47</sup>H. Vihola, A. Laukkanen, L. Valtola, H. Tenhu, and J. Hirvonen, *Biomaterials* **26**, 3055 (2005).
- <sup>48</sup>A. S. Wadajkar, B. Koppolu, M. Rahimi, and K. T. Nguyen, *J. Nanopart. Res.* **11**, 1375 (2009).
- <sup>49</sup>P. C. Naha, K. Bhattacharya, T. Tenuta, K. A. Dawson, I. Lynch, A. Gracia, F. M. Lyng, and H. J. Byrne, *Toxicol. Lett.* **198**, 134 (2010).
- <sup>50</sup>F. J. Xu, Y. Zhu, F. S. Liu, J. Nie, J. Ma, and W. T. Yang, *Bioconjugate Chem.* **21**, 456 (2010).
- <sup>51</sup>T. Takamoto, K. Yasuda, T. Tsujino, S. Sugihara, S. Kanaoka, S. Aoshima, and Y. Tabata, *J. Biomater. Sci. Polym. Ed.* **18**, 1211 (2007).
- <sup>52</sup>D. Le Garrec, J. Taillefer, J. E. Van Lier, V. Lenaerts, and J. C. Leroux, *J. Drug Target* **10**, 429 (2002).
- <sup>53</sup>R. W. Holley and J. A. Kiernan, *Proc. Natl. Acad. Sci. U.S.A.* **60**, 300 (1968).
- <sup>54</sup>D. R. Nisbet, J. S. Forsythe, W. Shen, D. I. Finkelstein, and M. K. Horne, *J. Biomater. Appl.* **24**, 7 (2009).
- <sup>55</sup>J. Yang, M. Yomato, K. Nishida, T. Ohki, M. Kanzaki, H. Sekine, T. Shimizu, and T. Okano, *J. Control Release* **116**, 193 (2006).
- <sup>56</sup>See supplementary material at <http://dx.doi.org/10.1116/1.4984933> for a video of the thermoresponsive behavior of espNIPAM.